Background-free millimeter-wave ultra-wideband signal generation based on a dual-parallel Mach-Zehnder modulator

Fangzheng Zhang and Shilong Pan*

Key Laboratory of Radar Imaging and Microwave Photonics, Ministry of Education Nanjing University of Aeronautics and Astronautics, Nanjing 210016, China
**pans@ieee.org*

Abstract: A novel scheme for photonic generation of a millimeter-wave ultra-wideband (MMW-UWB) signal is proposed and experimentally demonstrated based on a dual-parallel Mach-Zehnder modulator (DPMZM). In the proposed scheme, a single-frequency radio frequency (RF) signal is applied to one sub-MZM of the DPMZM to achieve optical suppressed-carrier modulation, and an electrical control pulse train is applied to the other sub-MZM biased at the minimum transmission point, to get an on/off switchable optical carrier. By filtering out the optical carrier with one of the first-order sidebands, and properly setting the amplitude of the control pulse, an MMW-UWB pulse train without the residual local oscillation is generated after photo-detection. The generated MMW-UWB signal is background-free, because the low-frequency components in the electrical spectrum are effectively suppressed. In the experiment, an MMW-UWB pulse train centered at 25 GHz with a 10-dB bandwidth of 5.5 GHz is successfully generated. The low frequency components are suppressed by 22 dB.

OCIS codes: (060.5625) Radio frequency photonics; (999.9999) Ultra-wideband (UWB); (999.9999) UWB-over-fiber.

References and links

1. D. Porcino and W. Hirt, "Ultra-wideband radio technology: potential and challenges ahead," IEEE Commun. Mag. **41**(7), 66–74 (2003).
2. FCC, "Revision of part 15 of the commission's rules regarding ultra-wideband transmission systems," 2–48, Arp. 2002.
3. M. Beltran, J. B. Jensen, X. Yu, R. Lorente, R. Rodes, M. Ortsiefer, C. Neumeyr, and I. T. Monroy, "Performance of a 60-GHz DCM-OFDM and BPSK-impulse ultra-wideband system with radio-over-fiber and wireless transmission employing a directly-modulated VCSEL," IEEE J. Sel. Areas Comm. **29**(6), 1295–1303 (2011).
4. M. Ran, B. I. Lembrikov, and Y. Ben Ezra, "Ultra-wideband radio-over-fiber concepts, technologies and applications," IEEE Photon. Journal **2**(1), 36–48 (2010).
5. S. Pan and J. P. Yao, "UWB over fiber communications: modulation and transmission," J. Lightwave Technol. **28**(16), 2445–2455 (2010).
6. Y. Yu, J. Dong, X. Li, and X. Zhang, "Photonic generation of millimeter-wave ultra-wideband signal using phase modulation to intensity modulation conversion and frequency up-conversion," Opt. Commun. **285**(7), 1748–1752 (2012).
7. Q. Chang, Y. Tian, T. Ye, J. Gao, and Y. Su, "A 24-GHz ultra-wideband over fiber system using photonic generation and frequency up-conversion," IEEE Photon. Technol. Lett. **20**(19), 1651–1653 (2008).
8. S. Fu, W. Zhong, Y. Wen, and P. Shum, "Photonic monocycle pulse frequency up-conversion for ultra-wideband-over-fiber applications," IEEE Photon. Technol. Lett. **20**(12), 1006–1008 (2008).
9. J. Li, Y. Liang, and K. K. Wong, "Millimeter-wave UWB signal generation via frequency up-conversion using fiber optical parametric amplifier," IEEE Photon. Technol. Lett. **21**(17), 1172–1174 (2009).
10. F. Zhang, J. Wu, S. Fu, K. Xu, Y. Li, X. Hong, P. Shum, and J. Lin, "Simultaneous multi-channel CMW-band and MMW-band UWB monocycle pulse generation using FWM effect in a highly nonlinear photonic crystal fiber," Opt. Express **18**(15), 15870–15875 (2010).
11. J. McKinney, "Background-free arbitrary waveform generation via polarization pulse shaping," IEEE Photon. Technol. Lett. **22**(16), 1193–1195 (2010).

#197831 - $15.00 USD Received 16 Sep 2013; revised 21 Oct 2013; accepted 25 Oct 2013; published 31 Oct 2013

12. T. Kuri, Y. Omiya, T. Kawanishi, S. Hara, and K. Kitayama, "Optical transmitter and receiver of 24 Ghz ultra-wideband signal by direct photonic conversion techniques," Int. Topical Meeting Microwave Photonics Grenoble, France, Oct. 2006.
13. Y. Du, J. Zheng, L. Wang, H. Wang, N. Zhu, and J. Liu, "Widely-tunbale and background-free ultra-wideband signals generation utilizing polarization modulation-based optical switch," IEEE Photon. Technol. Lett. **25**(4), 335–337 (2013).
14. L. X. Wang, W. Li, J. Y. Zheng, H. Wang, J. G. Liu, and N. H. Zhu, "High-speed microwave photonic switch for millimeter-wave ultra-wideband signal generation," Opt. Lett. **38**(4), 579–581 (2013).
15. L. Yan, W. Jian, J. Yu, K. Deming, L. Wei, H. Xiaobin, G. Hongxiang, Z. Yong, and L. Jintong, "Generation and performance investigation of 40GHz phase stable and pulse width-tunable optical time window based on a DPMZM," Opt. Express **20**(22), 24754–24760 (2012).

1. Introduction

Ultra-wideband (UWB) radio technology has been considered as a promising solution for short-range wireless communications and senor networks. The major advantages of the UWB technology include high data-rate capability (>1 Gb/s), low power consumption and low cost [1]. According to the definition of the U.S. Federal Communications Committee (FCC), a UWB signal should have a 10-dB bandwidth larger than 500 MHz or a fractional bandwidth greater than 20% with a power spectral density (PSD) no more than −41.3 dBm/MHz [1]. FCC also allocates the 3.1-10.6 GHz and 22-29 GHz bands for UWB wireless indoor communications and vehicular radar applications, respectively [2]. In addition, UWB in the 60 GHz band is emerging as an attractive approach for multi-Gb/s wireless communications [3]. To extend the coverage of UWB systems, UWB-over-fiber is proposed and has been proved to be a cost-effective solution [4, 5]. In the UWB-over-fiber systems, photonic generation, modulation, and distribution of UWB signals are highly desirable. To generate millimeter-wave (MMW) UWB signals in the 24- or 60-GHz band, several approaches have been demonstrated by up-converting a baseband UWB signal to the MMW band. The frequency up-conversion can be realized through a Mach-Zehnder modulator (MZM) [6, 7], or based on the nonlinear effects in a semiconductor optical amplifier (SOA) [8] or highly nonlinear fibers [9, 10]. The major drawback of the above techniques is that a strong local oscillation (LO) and many low-frequency components exist in the electrical spectrum of the generated signal. The strong residual LO component will reduce the energy efficiency or the transmission distance of the MMW-UWB system, and the low-frequency components, originated from the baseband UWB signal and also known as "background" [11], will disturb the narrow-band applications operated at the same frequency band. In order to generate background-free MMW-UWB signals without strong residual LO, several approaches have been demonstrated [12–14]. For example, two polarization modulators and an optical filter are used as a microwave photonic switch that truncates a sinusoidal MMW signal into short MMW-UWB pulses [14]. However, the complexity and stability of these systems need to be improved because multiple modulators, polarization devices and fiber-based interferometer structure are involved.

In this paper, we propose and experimentally demonstrate a compact and cost-effective scheme for background-free and LO-suppressed MMW-UWB signal generation using a dual-parallel MZM (DPMZM). An RF signal and an electrical control pulse train are applied to the two sub-MZMs of the DPMZM, respectively. The optical carrier and one of the first-order sidebands are filtered out by an optical filter. By properly setting the bias voltages of the two sub-MZMs and the amplitude of the electrical control pulses, a background-free MMW-UWB signal with suppressed LO is generated. The proposed scheme has simple structure and high stability since only one modulator is used. An experiment is performed. A 25-GHz background-free MMW-UWB signal with a 10-dB bandwidth of 5.5 GHz is generated. No strong residual LO component is observed in the electrical spectrum and the low-frequency components are suppressed by 22 dB.

#197831 - $15.00 USD Received 16 Sep 2013; revised 21 Oct 2013; accepted 25 Oct 2013; published 31 Oct 2013

2. Operation principle and numerical simulation

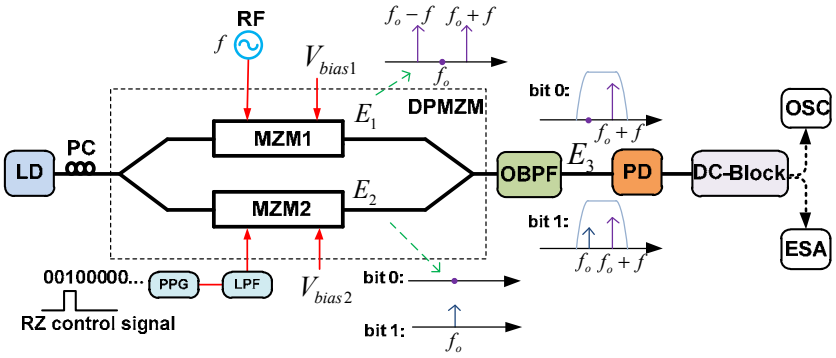

Fig. 1. Schematic diagram of the proposed MMW-UWB signal generator. LD: laser diode, PC: polarization controller, PPG: pulse pattern generator, LPF: electrical low-pass filter OBPF: optical band-pass filter, PD: photo-detector, OSC: oscilloscope, ESA: electrical spectrum analyzer.

Figure 1 shows the schematic diagram of the proposed MMW-UWB signal generation scheme. A continuous wave (CW) light from a laser diode (LD) is sent to a DPMZM. The DPMZM consists of two sub-MZMs (MZM1 and MZM2) embedded in the two arms of a parent MZM. There are two RF inputs and two independent DC bias voltages for the two sub-MZMs, respectively. The CW light introduced to the DPMZM is firstly split into two equal parts and then modulated at MZM1 and MZM2, respectively. MZM1 is biased at the minimum transmission point and is driven by a single-frequency RF signal, so optical suppressed-carrier modulation is performed which generates two first-order sidebands only when the RF signal power is small. The optical field after MZM1 can be written as

$$E_1 = A\exp[j2\pi(f_o - f)t] + A\exp[j2\pi(f_o + f)t], \tag{1}$$

where A is the amplitude of each sideband, f_o is the frequency of the optical carrier and f is the frequency of the RF signal. MZM2 is also biased at the minimum transmission point, but it is driven by an electrical control signal. The optical field after MZM2 is expressed as [15]

$$E_2 = B\exp(j2\pi f_o t) \propto \sin[\pi V/(2V_\pi)]\exp(j2\pi f_o t), \tag{2}$$

where V is the voltage of the control signal applied to MZM2, and V_π is the half-wave voltage of MZM2. The control signal is a return-to-zero (RZ) signal which can be regarded as a pulse train with one bit of '1' followed by several bits of '0', as shown in Fig. 1. To switch off and on the optical carrier, bit '0' is set to be a zero voltage and bit '1' is a nonzero voltage no more than V_π. By changing the voltage for bit '1', the amplitude of the optical carrier at the output of MZM2 can be adjusted. At the output of the DPMZM, an optical field that equals to the summation of E_1 and E_2 is obtained. An optical band-pass filter (OBPF) is connected to the DPMZM to remove one of the first-order sidebands. The optical field is then given by

$$E_3 = \begin{cases} A\exp[j2\pi(f_o - f)t] & bit\,'0' \\ A\exp[j2\pi(f_o - f)t] + B\exp(j2\pi f_o t) & bit\,'1'\,, \end{cases} \tag{3}$$

When this optical signal is sent to a photo-detector (PD) for square-law detection, the output current is

$$I(t) = \Re E_3 E_3^* = \begin{cases} \Re A^2 & bit\,'0' \\ \Re(A^2 + B^2) + 2\Re AB\cos(2\pi ft) & bit\,'1'\,, \end{cases} \tag{4}$$

#197831 - $15.00 USD Received 16 Sep 2013; revised 21 Oct 2013; accepted 25 Oct 2013; published 31 Oct 2013

where $\Re$ is the responsivity of the PD. By setting the amplitude of the electrical control signal to let $A >> B$ (e.g. $A \geq 10B$), $A^2 + B^2 \approx A^2$ is satisfied, so Eq. (4) is simplified to be

$$I(t) \approx \begin{cases} \Re A^2 & bit\,'0' \\ \Re A^2 + 2\Re AB\cos(2\pi ft) & bit\,'1' \end{cases}, \tag{5}$$

In Eq. (5), the output for bit '0' is a DC current, and that for bit '1' is an MMW pulse centered at *f*. This MMW pulse is biased at the same DC current as that for bit '0'. To obtain an MMW-UWB signal, the frequency of the RF signal and the pulse width for bit '1' should be carefully chosen to let the spectrum around *f* agree with the FCC regulations. Since the waveform corresponding to bit '0' is a DC term, residual LO component should not exist. Besides, the MMW-UWB pulse has equal amplitudes above and below the DC level, thus there are no low-frequency components in the spectrum, which means that the obtained MMW-UWB signal is background-free. The DC component in Eq. (5) can be removed simply using an electrical DC-block. If *B* is larger than or comparable to *A*, the DC terms for bit '0' and bit '1' in Eq. (4) are different, i.e., a pedestal exists for each MMW-UWB pulse. In this case, low-frequency components will appear in the electrical spectrum [11]. The proposed scheme is also suitable for UWB-over-fiber systems because the optical signal in Eq. (3) is an optical single sideband modulation (OSSB) signal containing only a modulated optical carrier and a first-order sideband. This feature is particularly favorable for the 60-GHz band MMW-UWB communication systems.

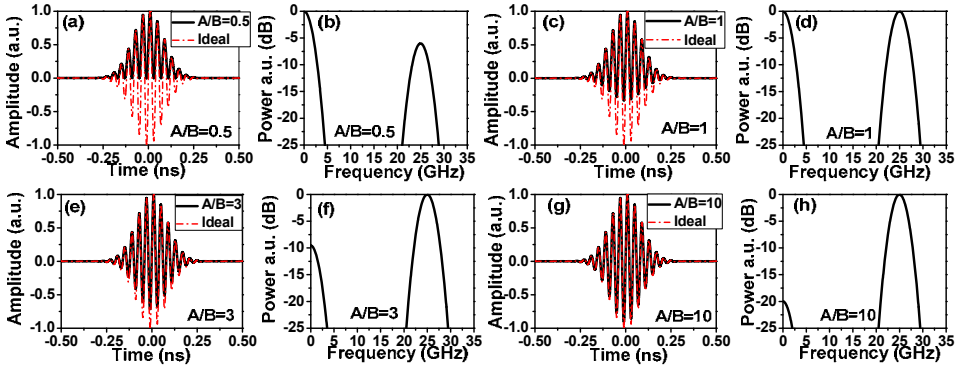

Fig. 2. Simulation results for the normalized waveforms and electrical spectra of the 25-GHz MMW-UWB pulses. (a) (b) A/B = 0.5, (c) (d) A/B = 1, (e) (f) A/B = 3 and (g) (h) A/B = 10.

Figure 2 shows the simulation results for a 25-GHz MMW-UWB signal generation using the proposed scheme. The frequency of the RF signal driving MZM1 is 25 GHz, and the control signal applied to MZM2 is a single Gaussian pulse with a full-width at half-maximum (FWHM) of 200 ps. By changing the amplitude of the electrical Gaussian pulse to let *A/B* be 0.5, 1, 3 and 10, respectively, the generated MMW-UWB pulses and the corresponding spectra are calculated and shown in Figs. 2(a)-2(h). For ease of comparison, the temporal waveform of an ideal background-free MMW-UWB pulse is also provided in Fig. 2. The ideal pulse has equal amplitudes above and below zero level, and its spectrum is centered at 25 GHz without residual LO and low-frequency components. When *A/B* = 0.5, the generated MMW-UWB pulse [Fig. 2(a)] is positive, and very strong low-frequency components with the peak power higher than that of the 25-GHz component is obtained [Fig. 2(b)]. When *A/B* = 1, the MMW-UWB pulse [Fig. 2(c)] has apparently unequal amplitudes above and below zero level. The corresponding spectrum [Fig. 2(d)] has strong low-frequency components that are comparable to the 25-GHz component. When *A/B* = 3, the amplitude below zero increases but is still smaller than that above zero [Fig. 2(e)]. The low frequency components in the spectrum are suppressed by about 10 dB compared with the 25-GHz component [Fig. 2(f)].

#197831 - $15.00 USD Received 16 Sep 2013; revised 21 Oct 2013; accepted 25 Oct 2013; published 31 Oct 2013

When A/B = 10, the pulse shape is close to the ideal pulse shape [Fig. 2(g)], and the low-frequency components are suppressed by about 20 dB. When A/B is further enlarged, the normalized pulse shape will be more close to the ideal background-free pulse, but the absolute amplitude of the MMW-UWB pulse reduces, because enlarging A/B is achieved by decreasing the value of B. To overcome this problem, an optical or electrical amplifier may be used to get the MMW-UWB pulses with a certain power level.

3. Experimental demonstration

An experiment is carried out based on the setup shown in Fig. 1. A CW light at 1550.1 nm is sent to a DPMZM (Fujitsu FTM7962EP) via a polarization controller (PC). The DPMZM has a half-wave-voltage of 3.5 V at 22 GHz. The two sub-MZMs are both biased at the minimum transmission point. MZM1 is driven by a 25-GHz RF signal, and MZM2 is driven by an electrical control signal generated by a pulse pattern generator (PPG), which has a date rate of 5 Gb/s and a fixed pattern of one '1' per 32 bits, corresponding to an RZ pulse train with a repetition rate of 156.25 MHz and a duty-cycle of 1/32. An electrical low-pass filter (LPF) with a bandwidth of 5-GHz is used to reshape the electrical control pulse to a Gaussian-like pulse. The above parameters can ensure that the spectral power of the generated MMW-UWB signal around 25 GHz is mainly located between 22 and 29 GHz, i.e., the frequency band for UWB vehicular radar applications. In addition, the two sub-MZMs are operated at the push-pull mode, such that chirp-free operation is implemented. After the DPMZM, a wavelength and bandwidth tunable OBPF (Yenista XTM-50) is inserted to select out the + 1st-order sideband and the optical carrier. Then, a 50 GHz PD is utilized to perform the optical-to-electrical conversion. A broadband electrical DC-block is followed to remove the DC component. The waveform of the generated MMW-UWB signal is observed through an oscilloscope (OSC, Agilent 86100A) and the spectrum is analyzed by an electrical spectral analyzer (ESA, Agilent E4447AU). In addition, an optical spectral analyzer (OSA) with a resolution of 0.02 nm is used to monitor the optical spectra.

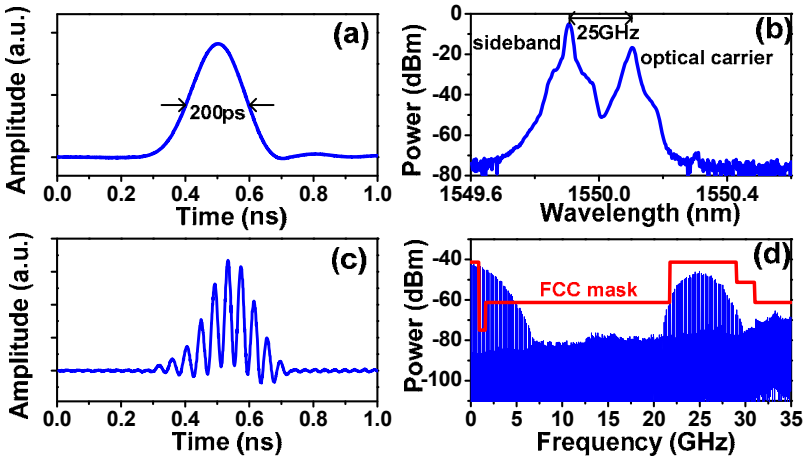

Fig. 3. (a) Waveform of the electrical control pulse, (b) the optical spectrum after the OBPF, (c) the waveform of the generated MMW-UWB pulse and (d) the electrical spectrum of the MMW-UWB pulse train.

Figure 3(a) shows the waveform of the electrical control pulse, of which the FWHM is about 200 ps. In the first step, the amplitude of the electrical control pulse is set to be a large value (2 V) such that A/B is a small value. Figure 3(b) shows the optical spectrum measured after the OBPF. The optical carrier and the + 1st-order sideband are filtered out and their frequency spacing is 25-GHz. The spectral power of the + 1st-order sideband is 11 dB higher than that of the optical carrier. The waveform of the generated MMW-UWB pulse is shown in Fig. 3(c), where a positive pedestal is obviously observed. The electrical spectrum of the

#197831 - $15.00 USD Received 16 Sep 2013; revised 21 Oct 2013; accepted 25 Oct 2013; published 31 Oct 2013

MMW-UWB pulse train and the FCC mask for UWB vehicular radar are shown in Fig. 3(d). As can be seen, an MMW-UWB signal around 25-GHz is generated without a strong residual LO component. However, the electrical spectrum does not conform to the FCC regulations, because strong low-frequency components below 5 GHz are generated. In this case, the obtained MMW-UWB signal is not background-free.

When the amplitude of the electrical control pulse is reduced, the MMW-UWB pulse shape becomes closer to a background-free waveform. Since the amplitude of the generated MMW pulse becomes smaller as *B* reduces, an erbium doped fiber amplifier (EDFA) is used before the OBPF. When an electrical control pulse with the amplitude of 0.22 V is applied, the experimental results are shown in Fig. 4. Figure 4(a) is the optical spectrum after the OBPF, where the spectral power of the + 1st-order sideband is 26 dB higher than that of the optical carrier. The waveform of the obtained MMW-UWB pulse shown in Fig. 4(b) has nearly equal amplitudes above and below zero. The corresponding electrical spectrum is shown in Fig. 4(c). The 10-dB spectral bandwidth around 25 GHz is measured to be 5.5 GHz and the low-frequency components are suppressed by 22 dB as compared to the 25 GHz component. Since the low-frequency components are effectively suppressed, the spectrum can easily satisfy the FCC mask, as shown in Fig. 4(c).

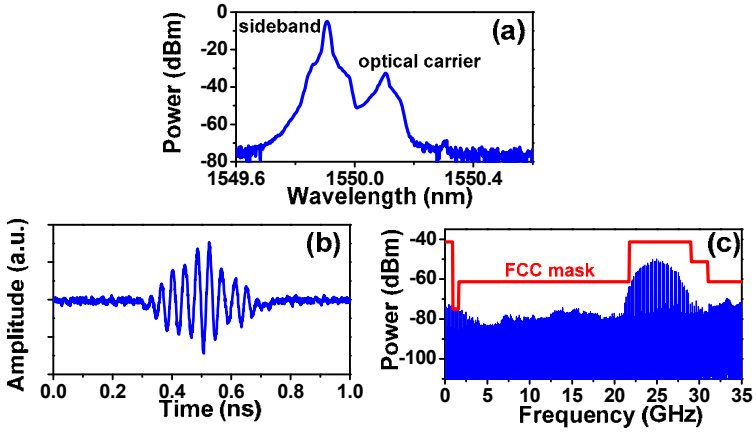

Fig. 4. (a): The optical spectrum after the OBPF, (b) the temporal shape of the generated MMW-UWB pulse and (c) the electrical spectrum of the MMW-UWB pulse train.

4. Conclusions

We have demonstrated a compact scheme for MMW-UWB signal generation using a DPMZM and an OBPF. By performing optical suppressed-carrier modulation in one of the sub-MZM and controlling the amplitude of the electrical pulse train applied to another sub-MZM, one of the first-order sidebands with an on/off switchable optical carrier were filtered out and sent to a PD for photo-detection. The obtained MMW-UWB signal had suppressed low-frequency components and no strong residual LO component. A 25-GHz background-free and LO-suppressed MMW-UWB signal was experimentally generated. The low-frequency components were suppressed by 22 dB.

Acknowledgments

This work was supported in part by the National Natural Science Foundation of China (61107063), the National Basic Research Program of China (2012CB315705), the Natural Science Foundation of Jiangsu Province (BK2012031), the Fok Ying Tung Education Foundation, the Fundamental Research Funds for the Central Universities (NE2012002, NP2013101), the Project sponsored by SRF for ROCS, SEM and a Project Funded by the Priority Academic Program Development of Jiangsu Higher Education Institutions.

#197831 - $15.00 USD Received 16 Sep 2013; revised 21 Oct 2013; accepted 25 Oct 2013; published 31 Oct 2013